Advanced Devices & Instrumentation
A SCIENCE PARTNER JOURNAL

RESEARCH ARTICLE

High-Performance Piezophototronic Solar Cells Based on Polarization Modulation Perovskite

Jiaheng Nie[1], Yaming Zhang[2], Lijie Li[3,*], and Yan Zhang[2,*]

[1]School of Cybersecurity, Chengdu University of Information Technology, Chengdu, China. [2]School of Physics, University of Electronic Science and Technology of China, Chengdu, China. [3]College of Engineering, Swansea University, Swansea, UK.

*Address correspondence to: l.li@swansea.ac.uk (L.L.); zhangyan@uestc.edu.cn (Y.Z.)

Citation: Nie J, Zhang Y, Li L, Zhang Y. High-Performance Piezophototronic Solar Cells Based on Polarization Modulation Perovskite. *Adv. Devices Instrum.* 2023;4:Article 0025. https://doi.org/10.34133/adi.0025

Submitted 24 July 2023
Accepted 17 September 2023
Published 28 September 2023

Polarization induced by electric field poling or strain can be used for achieving high-performance piezophototronic solar cell by tuning spatial surface potential distribution. Recent experiments presented that performance of perovskite solar cells (PSCs) can be enhanced with poling process due to surface state modification. Here, we characterize the effect of polarization on surface potential distribution of perovskite film, highlighting that piezophototronic effect provides a promising approach for enhancing the performance of PSCs. This method not only paves a new way to develop highly efficient perovskite photovoltaic devices but also designs highly stable PSCs.

Introduction

Many strategies are used to improve the performance of their PSC devices, including compositional engineering, solvent engineering, structural engineering, and interface engineering [1–5]. These strategies aim at optimizing their carrier generation and transportation processes, or constructing an efficient transport path of carriers, to suppress the recombination in the solar cell. Sargent and colleagues [6] found that a more uniform surface potential distribution of perovskite film, by modifying surface states, can maximize voltage in all-perovskite tandems, reduce effectively open-circuit voltage (V_{OC}) deficit, and achieve over power conversion efficiency (PCE) of 27% and V_{OC} of 2.19 V. The V_{OC} deficit of perovskite stems from V_{OC}-limiting recombination between the carrier transport layer and the perovskite layer [7,8]. This recombination is related to trap density of the perovskite surface [9]. Treating the perovskite surface energetics with dipoles of doped short-chain diammonium ligands contributes to the reduced interfacial recombination and surface homogeneity and promotes to improve PCE of the solar cell [6].

Polarization induced by electric field poling can achieve a uniform spatial surface potential distribution of perovskite film. Yang and colleagues [10] reported that an effective strategy for reducing trap states and regulating the surface potential by poling process after doping polarized ferroelectric polymers P(VDF-TrFE) leads to a significant decrease in voltage loss of 0.14 V. Previous work fabricated a piezophototronic perovskite solar cell (PSC) and found that the uniform surface potential distribution promoted by high polarization of ferroelectric polymers enables PCE of PSCs from 20.3% to 22.1% [11]. Polarization induced by strain also regulates the interface barrier by affecting perovskite surface states [12]. Li and colleagues [13] fabricated a PSC by doping ferroelectric material (PVDF:DH) with high polarizability, and the polarization of PVDF:DH suppresses the nonradiative recombination and increases the PCE to 24.2%. Zou and colleagues [14] doped a homochiral molecular ferroelectric in fabricated perovskite film to tune surface potential for facilitating effective charge transportation.

The piezophototronic effect is that polarization significantly tunes the generation, separation and transportation, and recombination processes of carriers at the semiconductor interface or contact [15,16], which shows strong vitality in the solar cell [17,18], photodetector [19,20], photocatalysts [21,22], and light-emitting diode (LED) [23,24]. The piezophototronic effect on perovskite materials can effectively modulate the separation, transportation, and recombination process of carriers in solar cell devices. Thus, the efficiency of piezophototronic PSCs can reach up to 22.1% from 20.3% by polarization [11]. The polarization induced by electric field poling process is used to promote the performance of PSCs. The positive or negative electric field poling process can lead to giant switchable photovoltaic effect, causing significant changes in the efficiency of PSCs [25]. In the case of external electric field poling or strain, a strong polarization field induced inside the cells changes the electric field behavior inside the light absorption layer or interface and drives the movement of carriers. Sun et al. [26] fabricated p-i-n structured hybrid PSCs using strain-enhancing device performance. Based on the piezophototronic effect, the piezoelectric potential induced by 1.88% strain effectively facilitated the carrier transport process, increasing the efficiency to 12.8%, an enhancement of about 40%. Additionally, Sun et al. [27] found that perovskite and polarization polymer thin films have sensitive ultraviolet responsiveness, which can be utilized for ultraviolet light detection and visualization. These films were used to fabricate multicolored fluorescent anti-counterfeiting tags, not only increasing the security dimensions of anti-counterfeiting but also having better stability compared to perovskite thin films [28].

In this work, the surface contact potential distribution of organic–inorganic halide perovskite composite films by doping P(VDF-TrFE) was investigated. We performed kelvin probe force microscopy (KPFM) measurement to study the surface potential map on perovskite composite films and to analyze the effect of spontaneous polarization on surface potential of composite films and found that adding an appropriate concentration of ferroelectric polymer helps to promote the uniform spatial distribution of surface potential. Piezophototronic PSCs decrease the volume of polarization. The spontaneous polarization generally occurs during the preparation of the device and is difficult to be well controlled. Moreover, the influence of spontaneous polarization on perovskite surface potential lacks enough understanding. Further analysis of the effect of polarization on the perovskite surface can provide guidance to further enhance the performance of PSCs. Our research presents the effect of spontaneous polarization on the surface potential, indicating that the polarization process is a key step for improving PCE in PSCs. Strain or electric field poling can help to form a highly ordered polarization by promoting uniform surface potential distribution and decreasing barrier height, efficiently enhancing the carrier transport process in PSCs.

Materials and Methods

Materials

Formamidinium iodide (FAI), methylammonium chloride (MACl), methylammonium bromide (MABr), and lead iodide (PbI_2) were purchased from Xi'an P-OLED Corp. (China). Dimethyl sulfoxide (DMSO) and *N*,*N*-dimethylformamide (DMF) were obtained from Sigma-Aldrich.

Film fabrication

The glass was cleaned ultrasonically by ultrapure water, acetone, and isopropanol after using detergent. The time for each cleaning is 20 min. Then, the substrate was treated with oxygen plasma to increase substrate wettability. Perovskite composite film was fabricated by two-step methods in the glove box filled with nitrogen gas. Perovskite precursor solution was prepared by dissolving PbI_2 and P(VDF-TrFE) powders in mixed solvent of DMF and DMSO, and the precursor solution temperature was kept at 60 °C for 8 h. After filtering, the glass substrate was spin-coated with perovskite precursor, followed by drying at 70 °C. Then, the mixed ammonium salt solution was used to form perovskite film by spin coating and annealing process, prepared by dissolving FAI, MACl, and MABr in isopropanol.

Thin-film characterization

A Rigaku-2500 x-ray diffractometer with x-ray tube (Cu Kα, $\lambda = 1.5406$ Å) was used for XRD patterns of perovskite composite film. Scanning electron microscopy (SEM) was performed on S-4800, Japan. The surface potential map is collected by KPFM (Dimension ICON, Bruker).

Results and Discussion

To achieve a more uniform spatial distribution of surface potential, Sargent and colleagues [6] introduced short-chain diammonium ligands to fabricate the perovskite films and modify perovskite surface states. Because surface dipoles induced by diammonium molecules can change energetics on the surface of perovskite films, they contributed to better energetic alignment at the interface of the perovskite layer and the carrier transport layer. Ferroelectric materials, with their asymmetric dipolar molecules and low processing temperature, are also ideal candidates for modifying the surface potential of perovskite [29]. P(VDF-TrFE) owns excellent ferroelectric properties, and orientation of the internal dipoles affects the local electric field. We fabricated the perovskite composite films by a two-step deposition strategy to observe the effect of polarization in P(VDF-TrFE) on perovskite films. The effect of P(VDF-TrFE) spontaneous polarization on morphology of composite films is observed by SEM. Figure 1A and B shows the surface morphology of untreated perovskite film and perovskite composite films at a scale of 1 μm. Although the two films both show relatively uniform and smooth morphology, compared with the untreated perovskite film, the perovskite composite film shows the large grain without damage. Figure S1 shows the SEM data of composite film doped with 0, 1, 2, and 4 mg of P(VDF-TrFE).

X-ray diffraction (XRD) profiles were used to offer an insight about crystal structure formation, degradation, and phase transformation. Figure 1C shows XRD data of perovskite composite materials. The diffraction peaks of perovskites occur at 14.1°, 24.5°, and 28.4°. The remaining PbI_2 produced by the two-step method has a peak at 12.8°. The β phase of P(VDF-TrFE) has a peak near 20°, which is shown in partial view of the XRD pattern. Compared to untreated perovskite films, the XRD data of perovskite composite film doped with 2 mg of P(VDF-TrFE) contain less PbI_2 and more perovskite. Based on XRD result of perovskite composite film, the doped P(VDF-TrFE) dipoles promote the crystallization of perovskite. Figure S2 shows the XRD data of composite film doped with 0, 1, 2, and 4 mg of P(VDF-TrFE). The composition of perovskite is $(FAPbI_3)_{1-y}(MAPbBr_{3-x}Cl_x)_y$, with the general formula of ABX_3, is shown in Fig. 1D, and the structure of β phase of P(VDF-TrFE) is shown in Fig. 1E. Figure 1F to H shows a schematic diagram of the piezophototronic effect on perovskite device performance [26]. The barrier height without polarization is shown in Fig. 1F. Strain or electric field poling-induced polarization can reduce negative carrier (electron) barrier height and increase positive carrier (hole) barrier height, as shown in Fig. 1G. PCE decreases under applied strain or electric field poling in this case. Alternatively, Fig. 1H shows that strain or electric field poling-induced polarization can reduce positive carrier (hole) barrier height and increase negative carrier (electron) barrier height; thus, PCE increases under applied strain or electric field poling.

In our previous works, we fabricated piezophototronic PSCs based on electric field poling process [11]. We experimentally characterized the key parameters for quantifying the performance enhancement of solar cells induced by polarization, including J_{SC} (short-circuit current density), V_{OC}, FF (fill factor), and PCE. The polarization induced by electric field poling can increase J_{SC} from 23.6 to 24.2 mA/cm^2, increase V_{OC} from 1.17 to 1.18 V, increase FF from 72.1 to 78.0, and improve PCE from 20.3% to 22.1%.

KPFM is used to characterize contact potential map and surface photovoltage of grain. KPFM characterizes the potential distribution from grain interior to grain boundaries (GBs) on the top surface of the films in the condition of dark or light [30]. Figure 2 shows the distribution of surface potential and topography map at grain and GB with a scale of 1 μm. Figure 2A shows the topography map probed by KPFM, and Fig. 2C shows the corresponding potential distribution map. Figure 2B presents the height and potential distribution along the white dotted line in Fig. 2A. Figure 2D shows the corresponding fitting curve. The

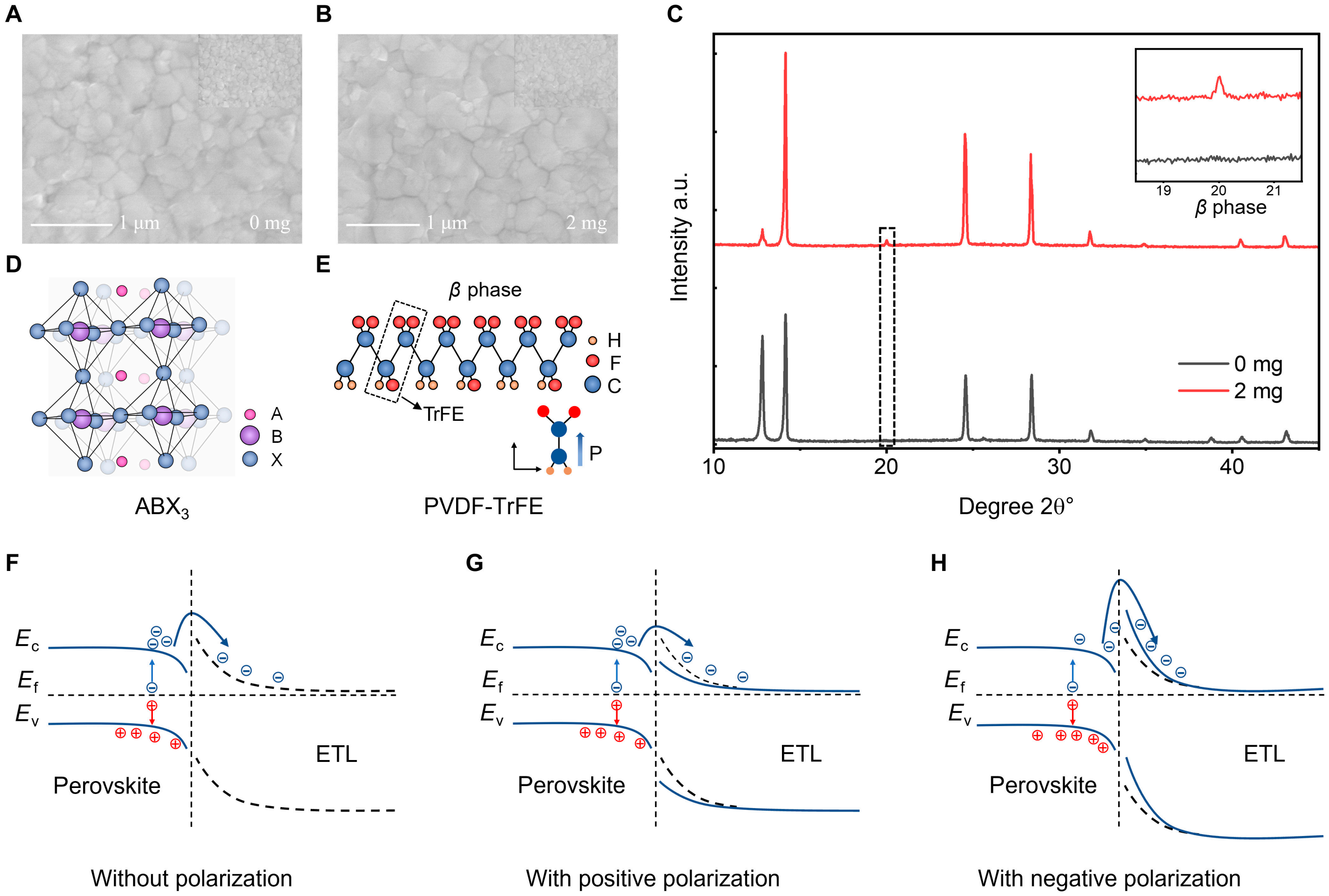

Fig. 1. SEM and XRD characterization of perovskite composite films, and molecule structures of perovskite and ferroelectric polymer. SEM image of perovskite films (A) and perovskite composite film (B). (C) XRD pattern of perovskite films and perovskite composite film. (D) Molecule structure of the perovskite adopting the ABX$_3$ form. (E) Molecule structures of P(VDF-TrFE). Schematic diagram of the piezophototronic effect modulating perovskite device performance without strain (F), with tensile strain (G), and with compressive strain (H).

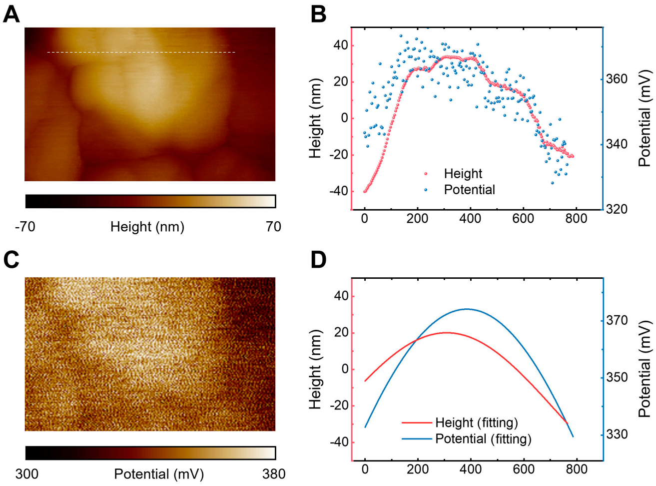

Fig. 2. The distribution of surface potential and topography map at grain and grain boundary. (A) Topography map with perovskite and P(VDF-TrFE) composite film. (B) Corresponding distribution of surface potential. (C) Height and potential distribution along the white dotted line. (D) Corresponding fitting curves.

switchable ferroelectric domains of organic–inorganic hybrid perovskite observed by piezo-response force microscopy (PFM) are equal to the grain in size [31]. As we have seen in Fig. 2, surface potential in grain is higher compared with that at the GBs. The separation process of carriers occurs in the grain, and then electrons and holes are transferred to the GB. A stable electric field induced by the spontaneous polarization behavior of perovskite in the grain locally promotes the separation and transportation process carriers.

To semiquantitatively describe the effect of polarization on surface characteristics of films, we used KPFM measurement to scan the surface potential distribution image of perovskite film. The experimental samples were fabricated by the same process and experimental conditions, and the only difference is the P(VDF-TrFE) content. We studied the polarization characteristics of composite film by characterizing the interfacial potential distribution of perovskite thin films. Figure 3 shows surface potential images and statistical data. The perovskite films doped with 0 mg of ferroelectric polymer own the potential with a distribution range of about 210 to 325 mV, as shown in Fig. 3A. The perovskite composite film doped with 2 mg of polarization polymer has the highest efficiency in the previous experiment [11]. Figure 3C presents the surface potential distribution image of composite film doped with 2 mg of polymer with a range of 400 to 500 mV. Figure 3B and D shows the statistical results of surface potential distribution, doped with 0 and 2 mg of ferroelectric polymer.

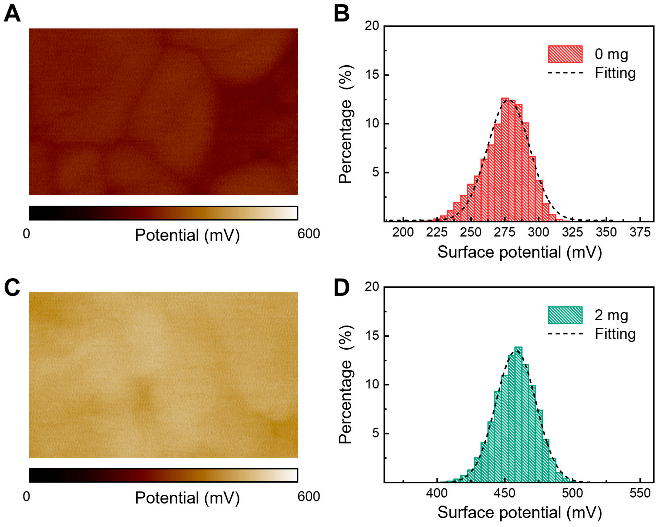

Fig. 3. The surface potential patterns with perovskite film (A) and P(VDF-TrFE) composite film (C). The statistical results of surface potential distribution with 0 mg (B) and 2 mg (D).

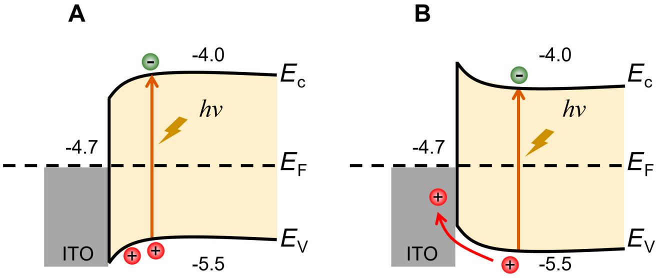

Fig. 4. Diagram of energy band between the perovskite layer and ITO. (A) Energy band state before polarization. (B) Energy band state after polarization.

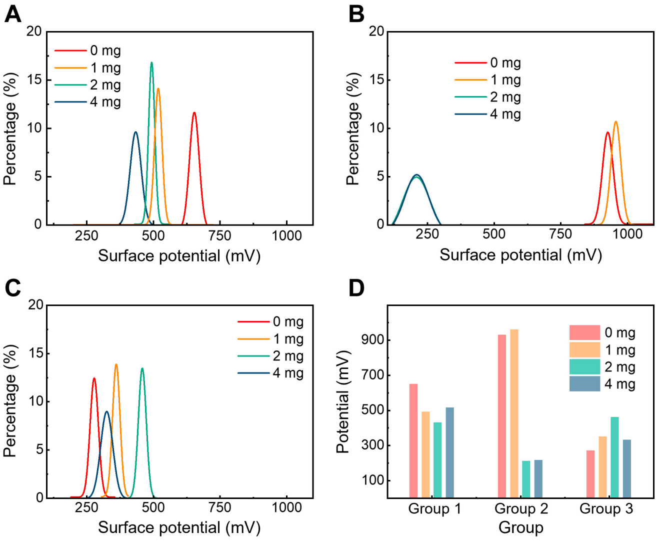

Fig 5. The surface potential statistical data of group 1 (A), group 2 (B), and group 3 (C). (D) Median surface potential of the composite film of three groups in the concentration of 0, 1, 2, and 4 mg of P(VDF-TrFE).

Figure 4 provides diagram of energy band between the perovskite layer and indium tin oxide (ITO) [32]. The energy band state before polarization is shown in Fig. 4A. The energy band bending of the interface that stemmed from polarization is shown in Fig. 4B. Polarization induced by external field can reconfigure interfacial energy band structure to selectively conduct holes while blocking the electron transportation, promoting an enhanced hole collection. This controllable polarization tuning surface potential or interfacial energy band can effectively manage the transportation process of carriers to promote PCE of cells.

The sample films produce spontaneous polarization behavior after fabrication. The samples for the experiment were divided into three groups, marked as group 1, group 2, and group 3. Each group contains four samples of perovskite composite film doped with 0, 1, 2, and 4 mg of polymer. Figure 5 shows surface potential distribution characteristics of films. Figure 5A to C shows the statistical data of surface potential with groups 1 to 3. The median surface potential of the composite film doped with 0, 1, 2, and 4 mg of P(VDF-TrFE) of groups 1 to 3 is shown in Fig. 5D. Due to the randomness of spontaneous polarization of composite films, the increase of polymer content is not positively or negatively correlated with the increase of surface potential, showing a random characteristic.

On the basis of the statistical data of surface potential from KPFM results in this work, the spontaneous polarization behavior of ferroelectric polymer can markedly affect surface potential of perovskite composite films. The random spontaneous polarization of perovskite composite films can lead to changes of potential distribution on the surface. In PSCs, uniform spatial potential distribution of the perovskite surface promotes less voltage loss, deeply affecting the carrier transport characteristics and the interface injection barrier. Therefore, controlling the polarization behavior of perovskite films can provide an effective way to regulate surface potential to enhance the carrier transport inside the solar cell. Based on piezophototronics, the highly ordered polarization formed by an applied electric field or strain can provide a reliable means to enhance the performance of PSCs.

Highly ordered polarization induced by strain or electric field poling can induce electric field aligned with the built-in electric field, leading to a noticeable drop in interfacial potential between the perovskite layer and the electron transport layer and inducing a significant band bending at the interface [33]. The polarization induced by electric field poling or strain can decrease interface carrier (hole) barrier height, promoting hole transport. Strain or electric field poling provides a new and simple approach to decrease interfacial barriers and enhance device performance, based on piezophototronic effect.

Polarization induced by electric field poling or strain can be used to tune surface potential and barrier height. When applying external electric field poling or strain, polarization generated within the device tunes the surface potential. Highly ordered polarization improves a more uniform surface potential distribution of cells by forming an additional electric field. The positive polarization can reduce hole barrier height at the interface and increase the PCE. The negative polarization can increase hole barrier height, reducing the PCE.

The device was fabricated by sequential deposition methods with a sandwich structure, consisting of Au, hole transport layer (HTL), perovskite layer, electron transport layer (ETL), and ITO. Electric field poling-induced polarization can provide external bias voltage between the two electrodes, and strain induces polarization by bending PSCs [10,11,26]. Strain or electric field poling-induced polarization can increase built-in potential, modulate barrier height, and promote carrier transport to improve PCE.

Modulating the surface potential of perovskite is an important step for enhancing device performance. Besides chemical methods, polarization can be used to control surface potential. The electric field poling or strain is performed on the entire device, and the electron and HTLs device is applied by the same polarization [10,11,14,26]. The highly ordered polarization induced by electric field poling or strain can reduce variations of surface potential, decreasing carrier barrier height and suppressing V_{OC}-limiting recombination at the interface [6,7]. The electric field poling or strain tune perovskite surface states improve the uniformity of the surface potential to enhance device performance.

Polarization improves device stability by modifying the surface potential distribution of the perovskite layer to form a uniform potential distribution. Nonuniform surface potential distribution can make organic–inorganic perovskite decompose in the presence of small molecules like water and oxygen, resulting in degradation of devices [34,35]. Jiang et al. [36] improved the uniformity of surface potential by controlling surface states, enabling stable device operation for over 2,400 h. Polarization induced by strain or electric field poling reducing potential gradients can prevent surface ion migration, maintain stable surface composition, and enhance device stability, based on piezotronic effect [6,35–37].

The piezophototronic effect utilizes the polarization induced by electric field poling or strain and modulates the interface barrier height and charge carrier transport properties. Sun et al. [26] modulated the carrier transport behaviors at the interface between the ZnO layer and the perovskite layer by strain to improve the efficiency by ~40%. Hu et al. [38] fabricated a PSC using a single ZnO nanowire and utilized polarization induced by strain at the two ends of the nanowire to regulate the photoelectric processes inside the device, including charge generation, separation, transport, and recombination, increasing PCE of the device from 0.0216% to 0.298%. Piezophototronics can enhance device performance by applying electric field poling or strain on solar cells without complicated fabrication procedure. Although current experiments have considered polarization orientation to quantify the effect of polarization on device performance, there are some challenges addressed in the research of polarization enhancing cell performance. The next steps of investigation need to characterize the potential profile across the perovskite cross-section to study changes in the interface electric field and barriers of PSCs before and after polarization. Meanwhile, future experiments also need to consider the effect of different polarization orientation angles on the surface potential of perovskite films, which impacts internal charge transport and device performance. PSC was typically fabricated by using spin-coating processes, and the next steps should also consider the impact of polarization on the electrochemical reactions during the perovskite film deposition process to further study the enhancement mechanism of polarization on PSCs.

Conclusion

In summary, the surface potential map of perovskite films was performed by KPFM device in this work. KPFM provides the potential distribution information by detecting the local contact potential of the perovskite surface. The statistical data of surface potential distribution indicate that controlling the uniformity of surface potential by optimizing polarization is a method for improving the PCE of PSC. The results show that polarization can change the surface potential distribution of the film, affecting the carrier transport process inside PSCs. Thus, the piezophototronic effect can provide an effective means for the efficiency enhancement of PSCs, by forming a highly ordered polarization inside the solar cell induced by external electronic field.

Acknowledgments

Funding: This work was supported by the Major Program of the National Natural Science Foundation of China (grant nos. 52192610 and 52192611), the Key Program of the National Natural Science Foundation of China (grant no. U22A2077), and the Fundamental Research Funds for the Central Universities (grant no. ZYGX2021YGCX001). **Author contributions**: J.N.: Methodology, formal analysis, data curation, writing—original draft, and validation. Yaming Zhang: Formal analysis and writing—original draft. L.L.: Formal analysis and writing—review and editing. Yan Zhang: Supervision, conceptualization, methodology, formal analysis, and writing—review and editing. **Competing interests**: The authors declare that they have no competing interests.

Data Availability

The data are available from the corresponding author on reasonable request.

References

1. Burschka J, Pellet N, Moon SJ, Humphry-Baker R, Gao P, Nazeeruddin MK, Gratzel M. Sequential deposition as a route to high-performance perovskite-sensitized solar cells. *Nature*. 2013;499(7458):316–319.
2. Jeon NJ, Noh JH, Kim YC, Yang WS, Ryu S, Seok SI. Solvent engineering for high-performance inorganic-organic hybrid perovskite solar cells. *Nat Mater*. 2014;13(9):897–903.
3. Zhou H, Chen Q, Li G, Luo S, Song TB, Duan HS, Hong Z, You J, Liu Y, Yang Y. Photovoltaics. Interface engineering of highly efficient perovskite solar cells. *Science*. 2014;345(6196):542–546.
4. Jeon NJ, Noh JH, Yang WS, Kim YC, Ryu S, Seo J, Seok SI. Compositional engineering of perovskite materials for high-performance solar cells. *Nature*. 2015;517(7535):476–480.
5. Shao Y, Yuan Y, Huang J. Correlation of energy disorder and open-circuit voltage in hybrid perovskite solar cells. *Nat Energy*. 2016;1:15001.
6. Chen H, Maxwell A, Li C, Teale S, Chen B, Zhu T, Ugur E, Harrison G, Grater L, Wang J, et al. Regulating surface potential maximizes voltage in all-perovskite tandems. *Nature*. 2023;613(6345):676–681.
7. Stolterfoht M, Wolff CM, Márquez JA, Zhang S, Hages CJ, Rothhardt D, Albrecht S, Burn PL, Meredith P, Unold T, et al. Visualization and suppression of interfacial recombination for high-efficiency large-area pin perovskite solar cells. *Nat Energy*. 2018;3:847–854.
8. Mahesh S, Ball JM, Oliver RDJ, McMeekin DP, Nayak PK, Johnston MB, Snaith HJ. Revealing the origin of voltage loss in mixed-halide perovskite solar cells. *Energy Environ Sci*. 2020;13:258–267.
9. Stolterfoht M, Caprioglio P, Wolff CM, Márquez JA, Nordmann J, Zhang S, Rothhardt D, Hörmann U, Amir Y, Redinger A, et al. The impact of energy alignment and interfacial recombination on the internal and external open-

circuit voltage of perovskite solar cells. *Energy Environ Sci*. 2019;12:2778–2788.

10. Zhang C-C, Wang Z-K, Yuan S, Wang R, Li M, Jimoh MF, Liao LS, Yang Y. Polarized ferroelectric polymers for high-performance perovskite solar cells. *Adv Mater*. 2019;31:e1902222.
11. Nie J, Zhang Y, Dan M, Wang J, Li L, Zhang Y. Piezophototronic effect enhanced perovskite solar cell based on P(VDF-TrFE). *Solar RRL*. 2021;5(12):2100692.
12. Nie J, Zhang Y, Li L, Wang J. Piezo-phototronic effect enhanced photodetectors based on $MAPbI_3$ perovskite. *J Mater Chem C*. 2020;8:2709–2718.
13. Chen W, Liu S, Li Q, Cheng Q, He B, Hu Z, Shen Y, Chen H, Xu G, Ou X, et al. High-polarizability organic ferroelectric materials doping for enhancing the built-in electric field of perovskite solar cells realizing efficiency over 24. *Adv Mater*. 2022;34:e2110482.
14. Xu XL, Xiao LB, Zhao J, Pan BK, Li J, Liao WQ, Xiong RG, Zou GF. Rational design of ferroelectric 2D perovskite for improving the efficiency of flexible perovskite solar cells over 23 %. *Angew Chem*. 2020;132:20149–20157.
15. Wang ZL. Nanogenerators, self-powered systems, blue energy, piezotronics and piezophototronics—A recall on the original thoughts for coining these fields. *Nano Energy*. 2018;54:477–483.
16. Zhu L, Wang ZL. Recent progress in piezo-phototronic effect enhanced solar cells. *Adv Funct Mater*. 2018;29(41):1808214.
17. Zhang Y, Yang Y, Wang ZL. Piezo-phototronics effect on nano/microwire solar cells. *Energy Environ Sci*. 2012;5:6850–6856.
18. Michael G, Zhang Y, Nie J, Zheng D, Hu G, Liu R, Dan M, Li L, Zhang Y. High-performance piezo-phototronic multijunction solar cells based on single-type two-dimensional materials. *Nano Energy*. 2020;76:105091.
19. Du X, Tian W, Pan J, Hui B, Sun J, Zhang K, Xia Y. Piezo-phototronic effect promoted carrier separation in coaxial p-n junctions for self-powered photodetector. *Nano Energy*. 2022;92:106694.
20. Zhu L, Lai Q, Zhai W, Chen B, Wang ZL. Piezo-phototronic effect enhanced polarization-sensitive photodetectors based on cation-mixed organic-inorganic perovskite nanowires. *Mater Today*. 2020;37:56–63.
21. Liu Z, Yu X, Li L. Piezopotential augmented photo- and photoelectro-catalysis with a built-in electric field. *Chin J Catal*. 2020;41(4):534–549.
22. Pan L, Sun S, Chen Y, Wang P, Wang J, Zhang X, Zou JJ, Wang ZL. Advances in piezo-phototronic effect enhanced photocatalysis and photoelectrocatalysis. *Adv Energy Mater*. 2020;10(15):2000214.
23. Xue X, Zang W, Deng P, Wang Q, Xing L, Zhang Y, Wang ZL. Piezo-potential enhanced photocatalytic degradation of organic dye using ZnO nanowires. *Nano Energy*. 2015;13:414–422.
24. Lei Y, Xu S, Ding M, Li L, Sun Q, Wang ZL. Enhanced photocatalysis by synergistic piezotronic effect and exciton–plasmon interaction based on $(Ag\text{-}Ag_2S)/BaTiO_3$ heterostructures. *Adv Funct Mater*. 2020;30(51):2005716.
25. Xiao Z, Yuan Y, Shao Y, Wang Q, Dong Q, Bi C, Sharma P, Gruverman A, Huang J. Giant switchable photovoltaic effect in organometal trihalide perovskite devices. *Nat Mater*. 2015;14(2):193–198.
26. Sun J, Hua Q, Zhou R, Li D, Guo W, Li X, Hu G, Shan C, Meng Q, Dong L, et al. Piezo-phototronic effect enhanced efficient flexible perovskite solar cells. *ACS Nano*. 2019;13:4507–4513.
27. Sun J, Li T, Dong L, Hua Q, Chang S, Zhong H, Zhang L, Shan C, Pan C. Excitation-dependent perovskite/polymer films for ultraviolet visualization. *Sci Bull*. 2022;67(17):1755–1762.
28. Sun J, Hua Q, Zhao M, Dong L, Chang Y, Wu W, Li J, Chen Q, Xi J, Hu W, et al. Stable ultrathin perovskite/polyvinylidene fluoride composite films for imperceptible multi-color fluorescent anti-counterfeiting labels. *Adv Mater Technol*. 2021;6(10):2100229.
29. Horiuchi S, Tokura Y. Organic ferroelectrics. *Nat Mater*. 2008;7:357–366.
30. Yun JS, Ho-Baillie A, Huang S, Woo SH, Heo Y, Seidel J, Huang F, Cheng YB, Green MA. Benefit of grain boundaries in organic–inorganic halide planar perovskite solar cells. *J Phys Chem Lett*. 2015;6(5):875–880.
31. Kutes Y, Ye L, Zhou Y, Pang S, Huey BD, Padture NP. Direct observation of ferroelectric domains in solution-processed $CH_3NH_3PbI_3$ perovskite thin films. *J Phys Chem Lett*. 2014;5:3335–3339.
32. Wu W-Q, Wang Q, Fang Y, Shao Y, Tang S, Deng Y, Lu H, Liu Y, Li T, Yang Z, et al. Molecular doping enabled scalable blading of efficient hole-transport-layer-free perovskite solar cells. *Nat Commun*. 2018;9:1625.
33. Zhang M, Chen Q, Xue R, Zhan Y, Wang C, Lai J, Yang J, Lin H, Yao J, Li Y, et al. Reconfiguration of interfacial energy band structure for high-performance inverted structure perovskite solar cells. *Nat Commun*. 2019;10:4593.
34. Zhu L, Wang L, Pan C, Chen L, Xue F, Chen B, Yang L, Su L, Wang ZL. Enhancing the efficiency of silicon-based solar cells by the piezo-phototronic effect. *ACS Nano*. 2017;11(12):1894–1900.
35. Tan S, Huang T, Yavuz I, Wang R, Yoon TW, Xu M, Xing Q, Park K, Lee D-K, Chen C-H, et al. Stability-limiting heterointerfaces of perovskite photovoltaics. *Nature*. 2022;605:268–273.
36. Jiang Q, Tong J, Xian Y, Kerner RA, Dunfield SP, Xiao C, Scheidt RA, Kuciauskas D, Wang X, Hautzinger MP, et al. Surface reaction for efficient and stable inverted perovskite solar cells. *Nature*. 2022;611(7935):278–283.
37. Li Z, Li B, Wu X, Sheppard SA, Zhang S, Gao D, Long NJ, Zhu Z. Organometallic-functionalized interfaces for highly efficient inverted perovskite solar cells. *Science*. 2022;376(6591):416–420.
38. Hu G, Guo W, Yu R, Yang X, Zhou R, Pan C, Wang ZL. Enhanced performances of flexible ZnO/perovskite solar cells by piezo-phototronic effect. *Nano Energy*. 2016;23:27–33.